

Design of a High Power MEMS Relay with Zero Voltage Switching and Isolated Power and Signal Transfer

Yan Zhang^{1,2}, Member, IEEE, Wenbo Liu¹, Lei Kou¹, Yan-Fei Liu¹, Fellow, IEEE, Chris Keimel³

¹Department of Electrical and Computer Engineering, Queen's University, Kingston, Canada

²Department of Electrical Engineering, Xi'an Jiaotong University, Xi'an, China

³Menlo Micro, Irvine, CA, USA

Email: zhangyanjtu@xjtu.edu.cn, liu.wenbo@queensu.ca, kou.lei@queensu.ca, yanfei.liu@queensu.ca, chris.keimel@menlomicro.com

Abstract—This paper proposes a MEMS relay circuit by paralleling an auxiliary MOSFET with a MEMS switch. During the turn-on and turn-off transition, MOSFET is turned on at first to guarantee the switching voltage of MEMS switch is almost zero; for normal switch-on condition the MEMS switch with low on-resistance is turned on and the MOSFET is turned off. To meet the requirement of isolation between control side and power side, a transformer is designed in the control circuit and this single transformer achieves both power transfer and on-off control signal transfer. Thus the size of MEMS relay is reduced. Finally, a prototype was built and it validates the design of MEMS relay structure and single transformer circuit. Superior switching performance, fast response, low on-resistance and small size are achieved by the MEMS relay.

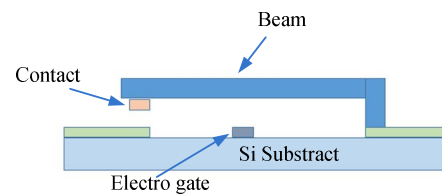
Keywords—MEMS relay; zero voltage switching; fast response;

I. INTRODUCTION

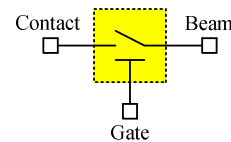
Electrical relay devices are widely used in any applications that require an isolated small signal to control high power circuit. The basic function of a relay is to switch on/off a high power circuit by an electrically isolated small power control signal. Electro-Mechanical Relay (EMR) driven by magnetic coils and Solid State Relay (SSR) based on silicon semiconductor device are the most commonly used types [1]-[3] in the industrial application. The former one is known for its low on-state resistance, high off-state voltage and large current capability while the latter for small size, mass producible, and easy on-chip integration. However, utilization of both types of relay has several obstacles. EMR suffers from the problems of metal-contact wear out, high voltage drive, and slow response time [4]. SSR has the relatively large on-resistance because it uses MOSFET as the conduction device and thus a large size of heat sink is needed to solve the thermal problem[5]. Furthermore, the opto-coupler which transfers the control signals in SSR limits the switching speed and slows the response.

MEMS switch is a device which has the advantages of SSR and EMR in low power applications. Until now, the great development of the metal device processing, high power system designs and the solid state micro switch fabrication

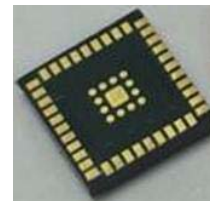
techniques significantly extends the power handling capability of MEMS switch [6][7]. Benefiting from this promising feature, MEMS switches can also be used in high power level. The existing MEMS switch with the minimum size of 5mm*5mm QFG package is shown in Fig.1. It is capable of carrying more than 3A current at 200V switching voltage while only consuming pico amperes of current. MEMS switch has the following obvious advantages in: a) low cost with surface micro-machining techniques, b) longer lifetime: more than 3 billion switching cycles; c) near zero power consumption and ultra-low insertion loss; d) easy to achieve multi-chips parallelism due to the positive temperature coefficient (on-state resistance of the MEMS switch with the higher current will



(a) Cross section of the physical structure.



(b) Single channel.



(c) Single chip.

Fig.1 MEMS switch structure, layout and prototype.

TABLE I Specification Comparison of Mechanical Relay, Solid State Relay and MEMS Relay of 200VDC rated voltage and 10A rated current.

Comparison items	EM Relay	Solid State Relay	MEMS Relay
On-state resistance	<100mΩ	<230mΩ	<50mΩ
ON/OFF switching time	>20ms	>1ms	<10us
Leakage current	75pA@200V	0.4mA@200V	75pA@200V
Switching operations	<30 million	<100 million	>3 billion

stabilized at the load current $i_{MOS}=i_{load}$.

Mode 4 (t_3-t_4): at t_3 , v_{PN} is almost zero $v_{PN}=0$. MEMS switch is turned on. i_{MOS} begins to decrease and i_{MEMS} starts to increase. In this switching on process, MEMS switch achieves zero voltage turn on. Until t_4 , MEMS switch is fully on state and the load current i_L is distributed in MEMS switch and MOSFET according to the on-state resistance.

Mode 5 (t_4-t_5): at t_4 , MOSFET is turned off. i_{MOS} is decreasing to zero. All the load current flows through MEMS switch until t_5 .

B. Switching OffTime Sequence

Mode 6 (t_6-t_7): at t_6 , the control signal v_{con} is coming to turn off the relay. G_{MOS} steps up immediately at t_7 to turn on MOSFET first.

Mode 7 (t_7-t_8): when MOSFET is turned on at t_7 , i_{MOS} begins to increase and i_{MEMS} starts to decrease. At t_8 , Both MEMS switch and MOSFET are conducting load current i_L .

Mode 8 (t_8-t_9): at t_8 , MEMS switch is turned off. v_{PN} is almost zero $v_{PN}=0$ because MOSFET is still conducting. i_{MEMS} decreases to zero at t_9 . The load current is flowing through MOSFET. During this switching off process, MEMS switch achieves zero voltage turn off.

Mode 9 (t_9-t_{10}): after a very small time delay until t_{10} , i_{MOS} is stabilized at the load current $i_{MOS}=i_{load}$.

Mode 10 ($t_{10}-t_{11}$): at t_{10} , MOSFET is turned off. i_{MOS} begins to decrease to zero and v_{PN} is increasing to the DC source voltage. At t_{11} , the relay is turned off. Selection of MOSFET

As an auxiliary component, the selection of MOSFET is a critical issue to guarantee that MEMS will be able to achieve the requirement of ZVS and also reduce the cost. Take consideration of the MEMS turn on process, a small enough R_{d_MOS} should be selected to ensure the switching voltage of MEMS switch V_{MOS_ON} is less than 0.5V to 1.0V at full load current after the MOSFET is turned on. The maximum on resistance follows the equation of (1):

$$R_{d_MOS} = \frac{V_{MOS_ON}}{I_{load_max}} \quad (1)$$

Where V_{MOS_ON} is MOSFET voltage drop under the maximum load current i_{Load_max} .

However, it is not necessary to minimize the MOSFET on resistance. Firstly, the contact resistance of MEMS is already very small, selecting a small on-resistance value will not decrease i_{MEMS} in Mode 7. Also, during t_3-t_4 and t_6-t_7 interval, the load current is distributed in MEMS switch and MOSFET according to the on-state resistance. We want the most of current flows across MEMS switch to keep a constant operating condition, thus R_{d_MOS} is supposed to be larger than R_{d_MEMS} . This actually allows the cost to be lower.

Furthermore, the auxiliary MOSFET switch almost has no power loss and works in relatively low frequency, thus a small package and low-cost MOSFET can be used. With the established MEMS relay, comparisons are made as shown in Table 1 and it can achieve much better performance than conventional SSR and ESR devices.

III. CONTROL CIRCUIT DESIGN WITH SINGLE TRANSFORMER

The compulsory isolation between control side and power side is required for MEMS relay [16-21]. Furthermore, the control circuit has the following requirements: a) transfer 5V on-off control command voltage to the MEMS switch and MOSFET gate signals in the secondary side. b) transfer 5V control voltage to 5V, 12V and 75V voltage in the secondary to provide power supply for control logic chip, MOSFET and MEMS switch driving circuit.

In order to minimize the relay size, an isolated circuit is proposed to acquire both secondary side power supply and on-off command information with single transformer. The diagram of control circuit is shown in Fig.4. As can be observed, when the turn-on control signal $v_{con}=5V$ is applied, pulse generator (such as LMC555) generates the 500kHz pulse waveform and then this signal is power amplified by ADP3624 as the primary side voltage of transformer. C_f is used to filter the DC component. The voltage doubling rectifying circuit including D_1 , D_2 , C_2 , C_3 is implemented to step up the transformer secondary voltage to the intermediate dc-link voltage $V_{cc}=6V$ which serves as the input of voltage regulation circuit. A high step-up DC-DC chip is used to generate 75V voltage for MEMS switch. A voltage doubler chip is used to generate 12V for MOSFET drive. And a linear voltage regulator is used as 5V power supply for the control circuit.

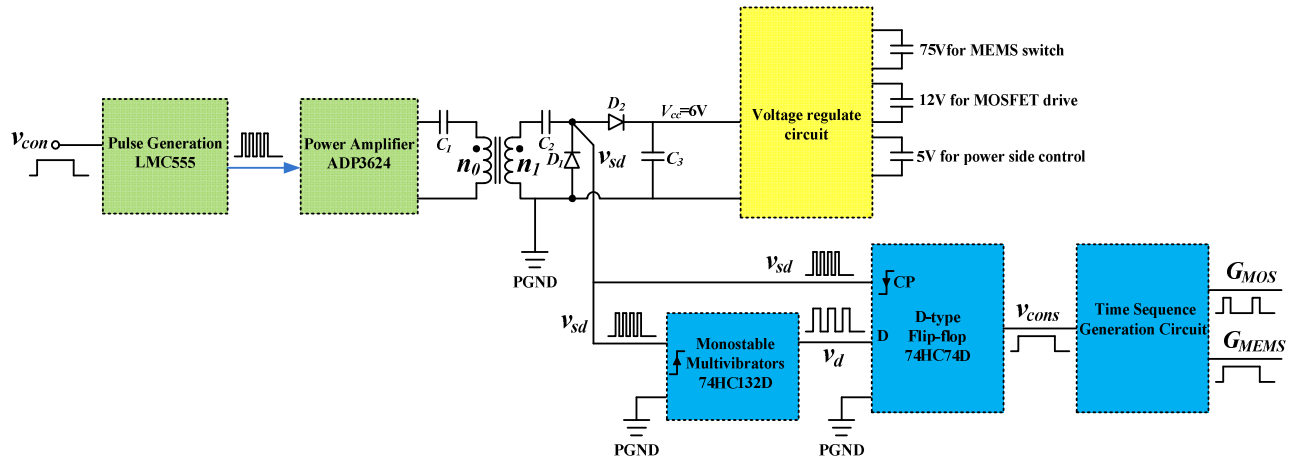


Fig.4 Control circuit diagram of MEMS relay.

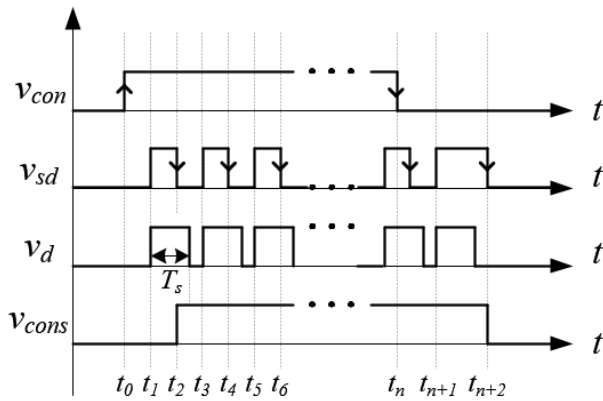


Fig.5 Operation principle of the control signal (v_{con}) detection circuit.

The secondary side also provides the MEMS relay on-off signal v_{sd} to the control circuit. The MEMS switch on/off signal v_{cons} in the secondary side is generated by a D-type flip-flop 74HC74D. v_{sd} is the trigger source (falling edge trigger) of the flip-flop, and the input (v_d) of the flip-flop is from the output of a monostable multivibrator 74HC132. Then, the time sequence circuit generates the gate control signal for MOSFET and MEMS switch according to operation principles of MEMS relay shown in Fig.3.

The detailed operation principle of control signal detection circuit is shown in Fig.5. Signals v_{sd} and v_d determine the on/off signal v_{cons} of MEMS switch by a D-type flip-flop, where v_d is the output of monostable multivibrator. The on-time of v_d is fixed ($T_s \approx 1/2f_s (min) = 1.25\mu s$). Signals v_{sd} and v_d shares the same rising edge.

1) When control signal v_{con} is high ($v_{con}=5V$), the frequency of v_{sd} is increased and its on-time is shorter than that of v_d . Therefore, when v_{sd} changes from high to low, v_d is still at high level. The falling edge of v_d triggers the D flip-flop so that the output of D flip-flop is always high ($v_{cons}=5V$) when the control signal v_{con} is high.

2) When control signal v_{con} is low ($v_{con}=0V$), the oscillating frequency of transformer decreases and the on-time of v_{sd} is longer than that of v_d . Therefore, when v_{sd} changes from high to low, v_d is low, and the output of D flip-flop goes to zero ($v_{cons}=0$).

By using the proposed control circuit, the signal and power isolation are achieved with only one transformer and the size of MEMS relay can be reduced.

IV. EXPERIMENT VERIFICATION

A. Test on the single MEMS prototype

The prototype of MEMS relay shown in Fig.6 was built to verify the improved switching performance from our circuit design and theoretical analysis. The paralleled MOSFET is mounted at the back side of MEMS. The studied case for a single MEMS relay is 200V/3A power capacity as maximum. MOSFET 18N55M5 with 550V maximum drain to source voltage, 16A drain current and 192m Ω on resistance is selected for experiment. The test condition is: $V_{dc}=50\sim 200V$, $R_{Load}=25\sim 100\Omega$ to obtain load current with different voltage conditions. The on resistance of MEMS $R_{d,MOS}$ is 70m Ω and the on resistance of selected auxiliary MOSFET is 192m Ω .

Fig.7 shows the waveforms of the MEMS relay during turn-on transition. The first channel is clock signal and its end time indicates the actual turn-on time of MEMS switch driver. The second channel shows the gate voltage of the MOSFET. The green curve is the total load current through the relay and the purple one is the voltage across the input and output terminals. It can be observed that the response time is only 30us and the voltage has already reached almost zero before MEMS switch turning on. Fig. 8 shows the waveforms while the relay is turn off transition and the response time is even shorter (20us). The 200V/2A on-off operation can be performed safely according to the figures. A snubber circuit is added to the prototype thus the current and voltage will change slowly after the MOSFET is turned off.

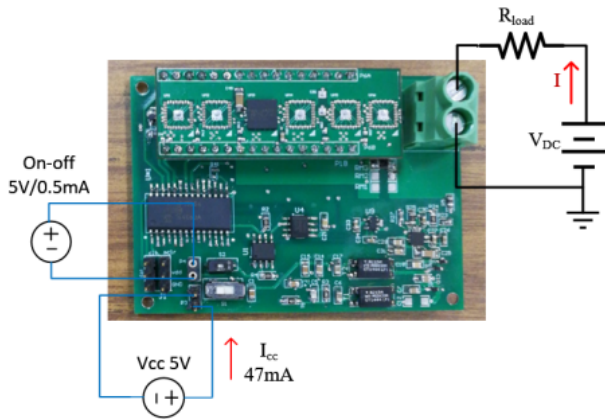


Fig.6 Prototype of MEMS relay

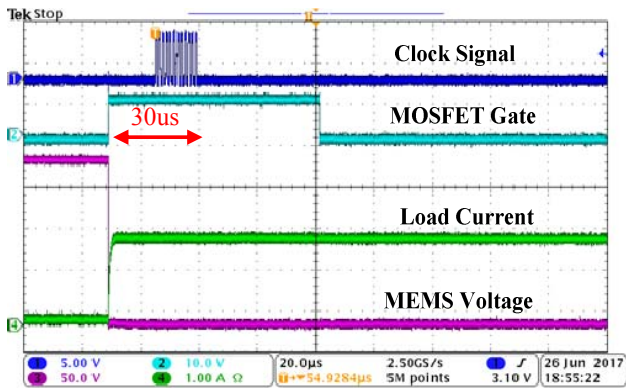


Fig.7 MEMS relay during turn-on transition.

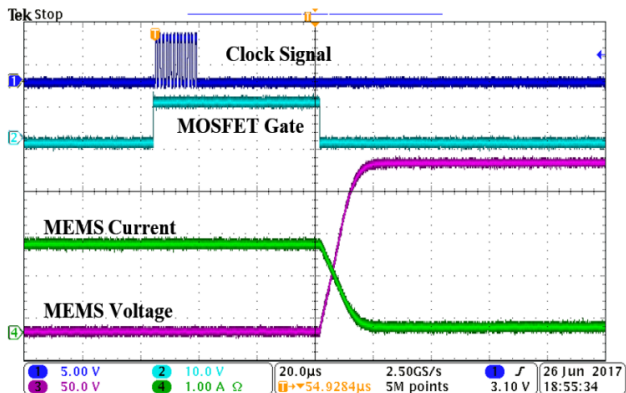


Fig.8 MEMS relay during turn-off transition.

Benefiting from the smart and fast response feature of the proposed MEMS relay, it can operate in switching mode at more than 1k Hz as shown in Fig.9. This feature also contributes to the fast over current protection, the MEMS switch can be shut down in a very short time when over current is detected. Fig. 10 and Fig. 11 demonstrate the waveforms in the protection procedure. The MOSFET is turned on as soon as load current hits the threshold as shown in Fig. 10 and then MEMS switch is turned off properly as the normal turn-off mode does.

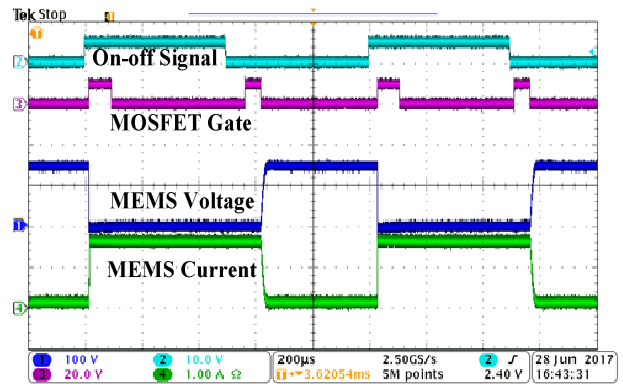


Fig.9 Signals of MEMS relay in on-off mode.

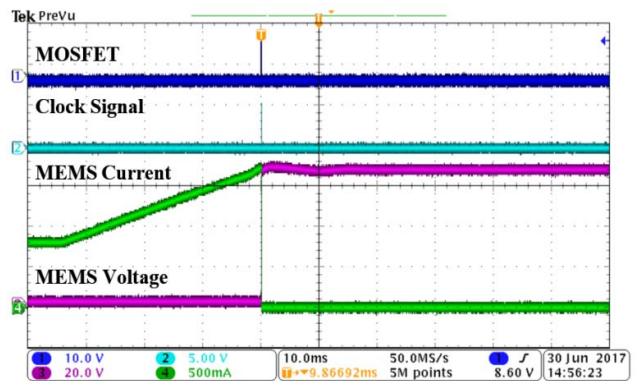


Fig.10 Over current protection in long time scale.

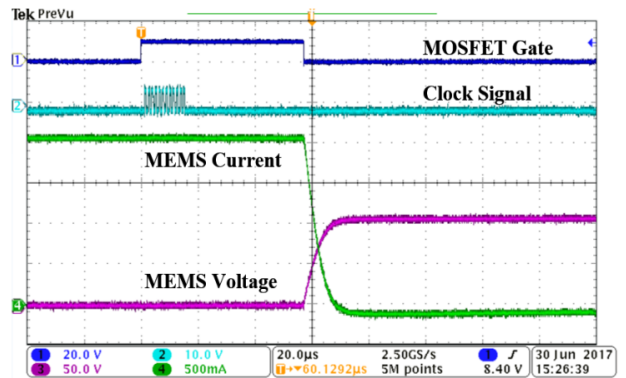


Fig.11 Over current protection in short time scale.

The voltage on the MEMS relay during the turn on and turn off transition are shown in Fig. 12 and Fig. 13. In period 1 of Fig. 12, when the MOSFET is on and MEMS is not on, the voltage drops to hundreds of millivolts; then during period 2, both MOSFET and MEMS are on and the voltage is a little lower; then in period 3 when the MOSFET is off MEMS voltage increases and reaches the input voltage. The oscillation occurs after MOSFET is turned on because large dv/dt is imposed and parasitic parameters draw this effect.

The voltage waveform is similar in turn off transition, it decreases in period 1 after the MOSFET is on and becomes

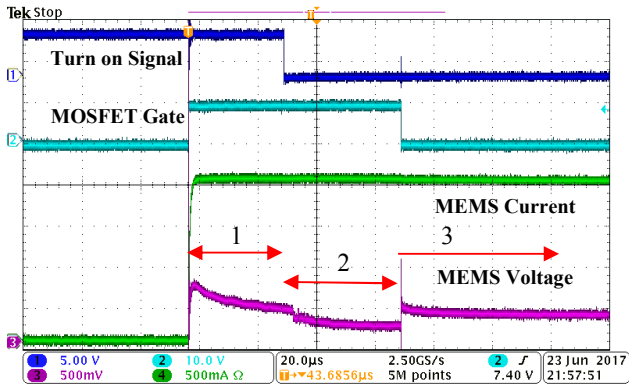


Fig.12 Detail MEMS during turn-on transition.

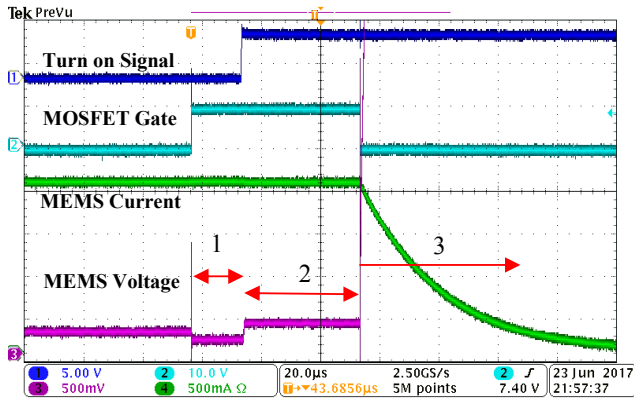


Fig.13 Detailed MEMS voltage during turn-off transition.

higher while the MEMS switch is off in period 2, then it rises after the MOSFET is turned off and the relay is off to shut down the power circuit. The oscillation is not as large as that in period 1, 2 and 3 in Fig. 12 because the dv/dt is much smaller thus the impact from parasitic parameters can be ignored.

B. Test on three-MEMS prototype

Another prototype with three MEMS switches and three MOSFETs in parallel is also built to test the performance with higher load current. The prototype is shown in Fig.14 and it is different from that in Fig. 6 by adding two pairs of MEMS switch and MOSFET on the top and bottom side of PCB. All the control signals are in parallel thus the three MOSFETs are turned on and off at the same time. Same condition happens to the MEMS switches.

It can be observed from Fig. 15 and Fig. 16 that the paralleled MEMS relays can be turned on and off safely with 4A load current at 100V input voltage. The MEMS switches are also turned on 30µs after the v_{cons} high signal arrives and can stay stable after the MOSFETs are turned off. During the transition the voltage drop is less than 1V therefore the switching energy of MEMS is very small.

On the parallel MEMS relay prototype, full load operation up to 10A current and its over current protection will be further investigated. Also the current sharing and thermal distribution characteristics will be studied.

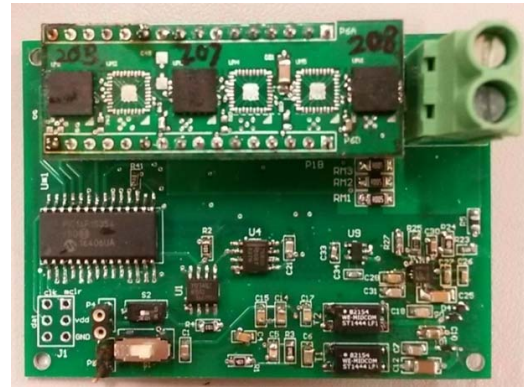


Fig.14 Three MEMS in parallel prototype.

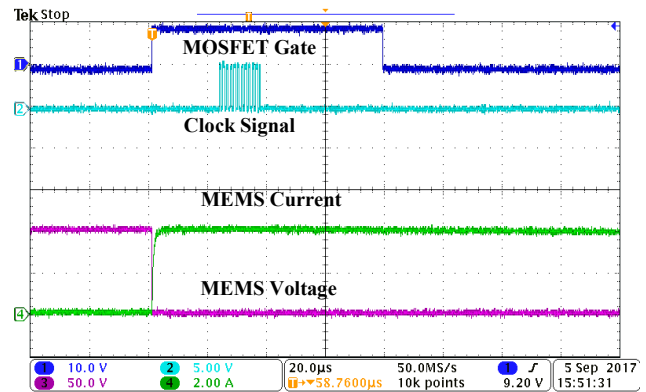


Fig.15 Waveforms during 3 MEMS turn-on transition.

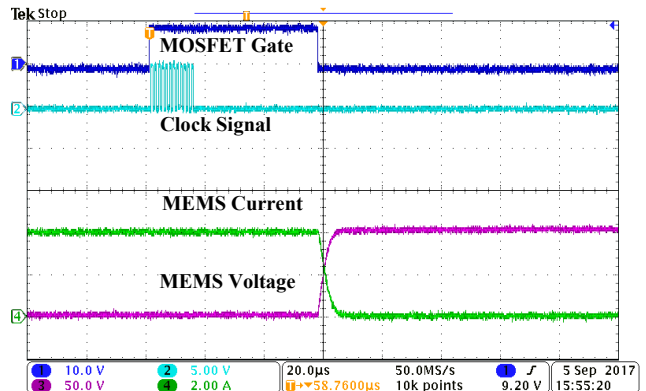


Fig.16 Waveforms during 3 MEMS relay turn-off transition.

V. CONCLUSION

The paper propose a novel MEMS based relay to achieve much better performance than conventional SSR and ESR. A paralleled auxiliary MOSFET is introduced to provide the zero voltage switching condition for MEMS switch. The ZVS condition significantly decrease the risk that may incur when the large voltage and current are overlapped during switching process. Furthermore, the control circuit uses only one transformer to minimize the relay size. Experimental results are performed and validate MEMS based relay can operate

under the serious switching condition with good performance. The voltage drop is less than 1V which effectively reduces the failure rate.

REFERENCES

- [1] Liu, Y., Bey, Y., & Liu, X. (2017). High-Power High-Isolation RF-MEMS Switches With Enhanced Hot-Switching Reliability Using a Shunt Protection Technique. *IEEE Transactions on Microwave Theory and Techniques*.
- [2] Liu, Y., Bey, Y., & Liu, X. (2016). Extension of the Hot-Switching Reliability of RF-MEMS Switches Using a Series Contact Protection Technique. *IEEE Transactions on Microwave Theory and Techniques*, 64(10), 3151-3162.
- [3] Yoon, Y. H., Song, Y. H., Ko, S. D., Han, C. H., Yun, G. S., Seo, M. H., & Yoon, J. B. (2016). A Highly Reliable MEMS Relay With Two-Step Spring System and Heat Sink Insulator for High-Power Switching Applications. *Journal of Microelectromechanical Systems*, 25(1), 217-226.
- [4] MKS-X-series relay datasheet. (2016) [Online] Available: <https://www.omron.com/>
- [5] Crydom DC400A10 datasheet. (2012) [Online] Available: <http://www.crydom.com/>
- [6] F. Copt, C. Koechli and Y. Perriard, "Electrostatically actuated MEMS relay for high power applications," 2016 19th International Conference on Electrical Machines and Systems (ICEMS), Chiba, 2016, pp. 1-6.
- [7] Y. H. Yoon et al., "A Highly Reliable MEMS Relay With Two-Step Spring System and Heat Sink Insulator for High-Power Switching Applications," in *Journal of Microelectromechanical Systems*, vol. 25, no. 1, pp. 217-226, Feb. 2016.
- [8] V. Agrawal, "A latching MEMS relay for DC and RF applications," *Proceedings of the 50th IEEE Holm Conference on Electrical Contacts and the 22nd International Conference on Electrical Contacts Electrical Contacts*, 2004., 2004, pp. 222-225.
- [9] Keimel, C., Claydon, G., Li, B., Park, J., & Valdes, M. E. (2012). Micro-Electromechanical-System based switches for power applications. *IEEE Transaction on Industry Applications*, 48(4), 1163-1169.
- [10] Keimel, C., Claydon, G., Li, B., Park, J., & Valdes, M. E. (2011, May). Micro-Electromechanical-System (MEMS) based switches for power applications. In *Industrial and Commercial Power Systems Technical Conference (I&CPS)*, 2011 IEEE (pp. 1-8). IEEE.
- [11] Krogstad, J. A., Keimel, C., & Hemker, K. J. (2014). Emerging materials for microelectromechanical systems at elevated temperatures. *Journal of Materials Research*, 29(15), 1597-1608.
- [12] Brand, V., Baker, M. S., & de Boer, M. P. (2013). Impact of contact materials and operating conditions on stability of micromechanical switches. *Tribology Letters*, 51(3), 341-356.
- [13] Bacon, P., Fischer, D., & Lourens, R. (2014). Overview of RF Switch Technology and Applications. *Microwave Journal*, 57(7).
- [14] Moran, T., Keimel, C., & Miller, T. (2016, October). Advances in MEMS switches for RF test applications. In *Microwave Conference (EuMC)*, 2016 46th European (pp. 1369-1372). IEEE.
- [15] Biskoping, M., Conrad, M., & De Doncker, R. W. (2015, March). Galvanically isolated driver using an integrated power-and signal-transformer. In *Industrial Technology (ICIT)*, 2015 IEEE International Conference on (pp. 1025-1030). IEEE.
- [16] Luz, P. C., Cosetin, M. R., Bolzan, P. E., Maboni, T., & do Prado, R. N. (2013, October). A family of isolated integrated drivers with reduced capacitors for light system based on power LEDs. In *Power Electronics Conference (COBEP)*, 2013 Brazilian (pp. 1114-1119). IEEE.
- [17] Naik, S., Shan, S., Umanand, L., & Reddy, S. (2017). A Novel Wide Duty Cycle Range Wide Band High Frequency Isolated Gate Driver for Power Converters. *IEEE Transactions on Industry Applications*.
- [18] Amiri, S. V. M., & Mirazizi, H. R. (2017, April). A new approach to optimal location of single-transformer sub-transmission substations using GIS analysis. In *Electrical Power Distribution Networks Conference (EPDC)*, 2017 Conference on (pp. 156-166). IEEE.
- [19] Choi, S. W., Lee, J. M., & Lee, J. Y. (2016). High-Efficiency Portable Welding Machine Based on Full-Bridge Converter With ISOP-Connected Single Transformer and Active Snubber. *IEEE Transactions on Industrial Electronics*, 63(8), 4868-4877.
- [20] Martins, A. S., Flores, G. C., & Barden, A. T. (2011, September). DC-DC and AC-DC voltage doubler boost converter for UPS applications. In *Power Electronics Conference (COBEP)*, 2011 Brazilian (pp. 601-606). IEEE.
- [21] Padilha, F. J., & Bellar, M. D. (2003, June). Modeling and control of the half-bridge voltage-doubler boost converter. In *Industrial Electronics, 2003. ISIE'03. 2003 IEEE International Symposium on (Vol. 2, pp. 741-745)*. IEEE.